

TRANSIENT PERFORMANCE EVALUATION OF WASTE HEAT RECOVERY RANKINE CYCLE BASED SYSTEM FOR HEAVY DUTY TRUCKS

Vincent Grelet^{a,b,c}, Thomas Reiche^a, Vincent Lemort^{b,*}, Madiha Nadri^c,
Pascal Dufour^c

^a*Volvo Trucks Global Trucks Technology Advanced Technology and Research, 1 av Henri
Germain 69800 Saint Priest, France, (vincent.grelet@volvo.com,
thomas.reiche@volvo.com).*

^b*LABOTHAP, University of Liege, Campus du Sart Tilman Bat. B49 B4000 Liege,
Belgium, (vincent.lemort@ulg.ac.be).*

^c*Universite de Lyon, F-69622, Lyon, France, Universite Lyon 1, Villeurbanne, France,
CNRS, UMR 5007, LAGEP, (nadri@lagep.univ-lyon1.fr, dufour@lagep.univ-lyon1.fr).*

Abstract

The study presented in this paper aims to evaluate the transient performance of a waste heat recovery Rankine cycle based system for a heavy duty truck and compare it to steady state evaluation. Assuming some conditions to hold, simple thermodynamic simulations are carried out for the comparison of several fluids. Then a detailed first principle based model is also presented. Last part is focused on the Rankine cycle arrangement choice by means of model based evaluation of fuel economy for each concept where the fuels savings are computed using two methodologies. Fluid choice and concept optimization are conducted taking into account integration constraints (heat rejection, packaging ...). This paper shows the importance of the modeling phase when designing WHRS and yields a better understanding when it comes to a vehicle integration of a Rankine cycle in a truck.

Keywords: Waste heat recovery system, Modeling, Thermodynamic,

*Corresponding author

1. INTRODUCTION

Even in nowadays heavy duty (HD) engines, which can reach 45% of efficiency, a high amount of the chemical energy contained in the fuel is released as heat to the ambient. Driven by future emissions legislation and increase in fuel prices, engine gas heat recovering has recently attracted a lot of interest. Over the last decades, most of the research has focused on waste heat recovery systems (WHRS) based on the Rankine cycle [? ? ?]. These systems can lead to a decrease in fuel consumption and lower engine emissions [? ?]. Recent studies have brought a significant potential for such systems in a HD vehicle [? ?]. However, before the Rankine cycle based system can be applied to commercial vehicles, the challenges of its integration have to be faced. The work done in [?] and [?] show that one of the main limitation is the cooling capacity of the vehicle. But other drawbacks, such as the back pressure, weight penalty or transient operation should not be minimized [? ?]. Before tackling the problem of the control strategy of this system [? ?], the architecture and components need to be selected to achieve a certain objective that could be to maximize the fuel savings or minimize the impact on the vehicle. This study focuses more on maximizing the system performance by taking into account the different penalties induced by the integration of the system on a heavy duty truck. Technical challenges and optimization of stationary ORC are well adressed [? ?] but for mobile applications only few studies deal with fuel saving potential of WHRS on dynamic driving cycles [? ?] and the latter is generally reduced to a certain number of steady state engine operating points [? ?]. This last approach leads to an overestimation of the WHRS performance [?] and therefore of the fuel economy. In [?] different concepts are analyzed taking into account the system integration into the vehicle cooling module. The concepts differ in the number of heat sources used and the temperature level of the cooling fluid. Each is simulated on different steady state engine operating points and the fuel economy is calculated taking into account the increase in cooling fan consumption, exhaust back pressure or intake manifold temperature. Depending on the Rankine configuration and the location of the condenser, improvements from 2.2% (recovering heat only from exhaust gases

34 and condenser placed in front of the cooling package) to 6.9% (exhaust gas
35 recirculation and exhaust heat are recovered and condenser is fed with engine
36 coolant) are achieved. In [?], dynamic fuel economy is evaluated on a light
37 duty vehicle taking into account the main penalties induced by the integra-
38 tion of the WHRS. Fuel savings from 3.4% to 1.3% are presented depending
39 on the level of integration of the system into the vehicle architecture. How-
40 ever, no optimization is proposed either on the system architecture or on the
41 condenser integration into the cooling package.

42 This paper is organized as follows. The second section explains the different
43 considerations to take when designing a Rankine cycle for a HD applica-
44 tion. In the third section, the different models used in the rest of the study
45 are explained. In the fourth section, the scope of the study and the differ-
46 ent methodologies are explained. In the fifth section, simulation results are
47 analyzed and possible improvements are proposed. Finally, conclusions are
48 drawn and directions for future research work are discussed.

49 2. DESIGN ASPECTS TO CONSIDER

50 Figure 1 shows a simple waste heat recovery system mounted on a 6 cylinder
51 heavy duty engine. Working fluid flows through four basic components which
52 are: the pump, the evaporator linked to the heat source, the expansion ma-
53 chine and the condenser linked to the heat sink. For sake of clarity, the link
54 between the expander and the engine driveline is represented by a dashed
55 line since it can be either mechanical or electrical (by coupling a generator to
56 the expansion machine and reinject the electricity on the on board network).

58 2.1. Working fluid choice

59 There are several aspects to take into account when choosing a working
60 fluid for this application. Unlike stationary power plants where the main
61 consideration is the output power or the efficiency, here other aspects have to
62 be considered such as fluid deterioration, environmental aspects or freezing.
63 Up to now, several studies have tried to identify the ideal fluid for WHRS
64 [? ? ?] but no single fluid has been found. Recently, new performance
65 indicators have been introduced [? ?], where cost and design issues enter
66 into consideration.

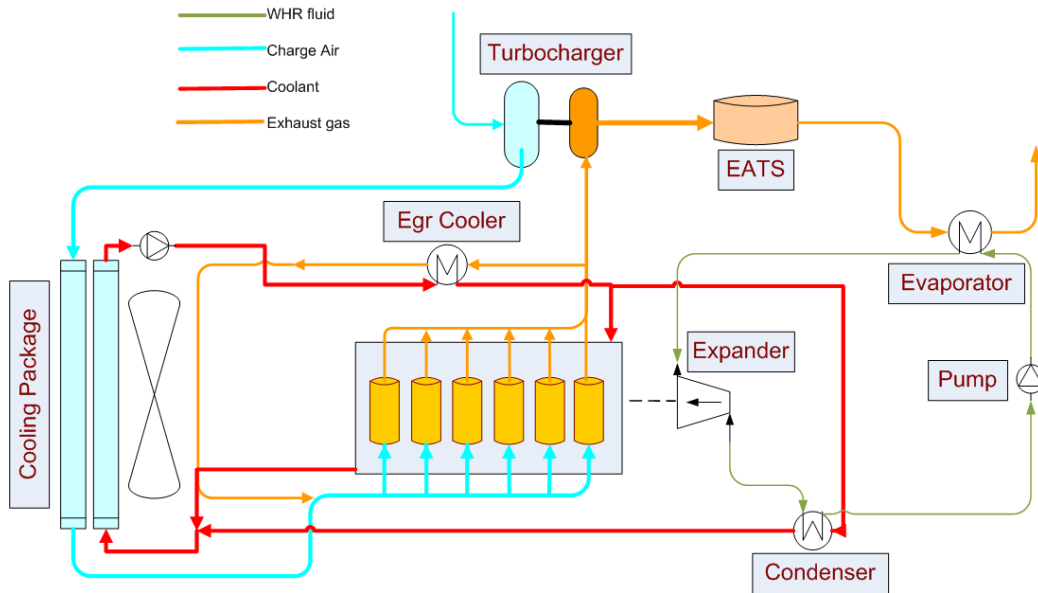


Figure 1: Simple waste heat recovery Rankine based system

67 *2.2. Heat sources*

68 On a commercial vehicle, a certain number of heat sources can be found
 69 such as exhaust gases, cooling water or engine oil. These ones have several
 70 grade of quality (temperature level) and quantity (amount of energy). If the
 71 number of heat sources often yields higher fuel savings, it also brings more
 72 complexity and more challenges for the design of the system (fluid, expansion
 73 machine, control).

74 *2.3. Heat sink*

75 On a HD Truck, the only heat sink available is the vehicle cooling package
 76 which is a module including radiators for the compressed air and the engine
 77 coolant and cooled down by means of the ram air effect and the cooling
 78 fan. Integration of a WHRS into the cooling module results on a higher load
 79 on the latter and limits the amount of waste heat that can be converted
 80 into useful work. As such, complete system analysis is necessary to find the
 81 optimal way of recovering heat from a vehicle.

82 2.4. Subsystem interaction

83 The engine operation is influenced by the introduction of a WHRS. For ex-
84 ample, as the WHRS shares the cooling system of the vehicle, the charge air
85 cooling capacity can be lower, which has a negative behavior on the engine
86 performance. Another example is the use of exhaust gas recirculation (EGR)
87 as heat source. This leads to a trade-off between EGR cooling and Rank-
88 ine cycle performance, which could impact negatively the engine emissions.
89 Several other interactions such as the exhaust back pressure or the weight
90 penalty could be cited.

91

92 The WHRS performance, and so the fuel economy induced by this later, is
93 then dependent on all these aspects. It is therefore critical to model the
94 complete system and its environment in order to optimize its architecture. It
95 helps to select the best design and reduce the number of experimental tests
96 to carry out.

97 3. RANKINE MODELING

98 3.1. Rankine process

99 The Temperature Entropy (T-s) diagram represented in figure 2 shows the
100 associated state changes of the working fluid through the Rankine cycle:

- 101 • The pressure of the liquid is increased by the pump work up to the
102 evaporating pressure ($1 \rightarrow 2$).
- 103 • The pressurized working fluid is pre-heated ($2 \rightarrow 3a$), vaporized ($3a \rightarrow$
104 $3b$) and superheated ($3b \rightarrow 3c$) in a heat exchanger, by recovering heat
105 (\dot{Q}_{in}) from the heat source.
- 106 • The superheated vapor expands from evaporating pressure to condens-
107 ing pressure ($3c \rightarrow 4$) in an expansion device creating mechanical power
108 (\dot{W}_{out}).
- 109 • The expanded vapor condenses ($4 \rightarrow 1$) through a condenser (linked to
110 the heat sink) releasing heat (\dot{Q}_{out}).

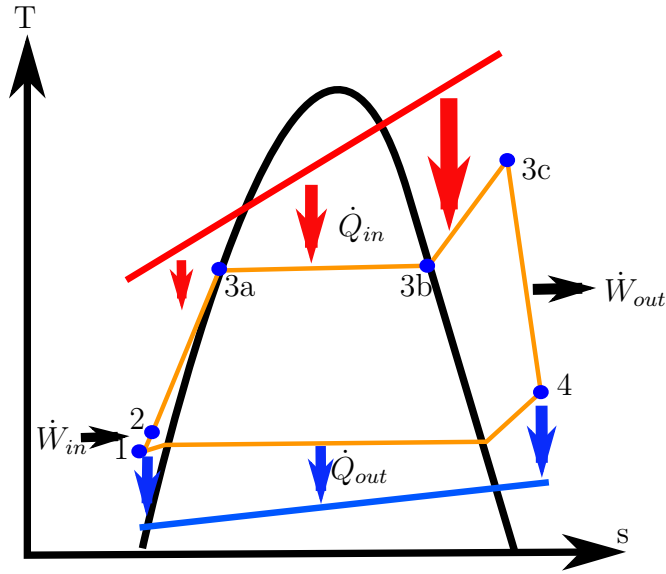


Figure 2: Temperature-Entropy diagram of the Rankine cycle

111 In this process the changes of states in both the pump and the expander are
 112 irreversible and increase the fluid entropy to a certain extent. To correctly
 113 assess the performance of a system based on the Rankine cycle, two different
 114 models have been developed: a simple 0D steady state model based on the
 115 enthalpy change that undergoes the working fluid which does not intend to
 116 represent components performance and where the dynamic is not taken into
 117 account and a second, based on conservation principles applied on one spatial
 118 dimension. This is required to represent real performance of the components
 119 constituting the system either in steady state or in transient.

120 3.2. 0D steady state modeling of a Rankine cycle

121 In order to simulate a high number of working fluids, a 0D model of a Rankine
 122 cycle using one heat source is developed. It does not represent a real system
 123 but it allows a fast assessment of a various number of working fluids. It
 124 helps to select the suitable working fluids for the studied application. This
 125 model is based on the enthalpy changes in the process described in section
 126 3.1. This model is able to perform either subcritical or supercritical cycle,
 127 which avoids the vaporization process and leads to a smaller system and a
 128 better heat recovery process [?]. Those relations are verified as long as

129 the heat losses in the system and in the components are neglected. The 0D
 130 model used is given by the system of equations (1):

$$\left\{ \begin{array}{l}
 P_{cond} = P_{sat}(T_{cond}), \\
 P_{fin,pump} = P_{cond}, \\
 T_{fin,pump} = T_{sat}(P_{fin,pump}) - \Delta T_{subcooling}, \\
 h_{fin,pump} = h(T_{fin,pump}, P_{fin,pump}), \\
 s_{fin,pump} = s(h_{fin,pump}, P_{fin,pump}), \\
 P_{fout,pump} = P_{evap}, \\
 h_{fout,pump} = h_{fin,pump} + \frac{(h_{fout,pump_{is}} - h_{fin,pump})}{\eta_{pump_{is}}}, \\
 T_{fout,pump} = T(h_{fout,pump}, P_{fout,pump}), \\
 s_{fout,pump} = s(h_{fout,pump}, P_{fout,pump}), \\
 P_{fout,boiler} = P_{fout,pump}, \\
 h_{fout,boiler} = h_{fout,pump} + \frac{\dot{Q}_{gas}}{\dot{m}_f}, \\
 T_{fout,boiler} = T(h_{fout,boiler}, P_{fout,boiler}), \\
 s_{fout,boiler} = s(h_{fout,boiler}, P_{fout,boiler}), \\
 P_{fout,exp} = P_{cond}, \\
 h_{fout,exp} = h_{fout,boiler} + (h_{fout,boiler} - h_{fout,exp_{is}})\eta_{exp_{is}}, \\
 s_{fout,exp} = s(h_{fout,exp}, P_{fout,exp}), \\
 P_{fout,cond} = P_{fout,exp}, \\
 T_{fout,cond} = T_{sat}(P_{fout,cond}) - \Delta T_{subcooling}, \\
 h_{fout,cond} = h(T_{fout,cond}, P_{fout,cond}), \\
 s_{fout,cond} = s(h_{fout,cond}, P_{fout,cond}).
 \end{array} \right. \quad (1)$$

where

$$\left\{ \begin{array}{l}
 h_{fout,pump_{is}} = h'(P_{fout,pump}, s_{fin,pump}), \\
 \dot{Q}_{gas} = \dot{m}_{gas} c_{p_{gas}} * (T_{gas_{in,boiler}} - T_{gas_{out,boiler}}), \\
 h_{fout,exp_{is}} = h'(P_{fout,exp}, s_{fout,boiler}), \\
 h_{fout,exp} \geq h''(x_{fout,exp_{min}}, P_{fout,exp}).
 \end{array} \right. \quad (2)$$

131 In table 1 one can find the simulation model parameters, and the abbrevia-
 132 tions are given in the appendix.

133 In addition to that, a routine verifying that the pinch point (PP) is respected
 134 during the evaporation process.

| Model parameters | Variable in (1) | unit | value |
|---------------------------------|---|------|-------|
| Pump isentropic efficiency | $\eta_{pump\,is}$ | % | 65 |
| Expander isentropic efficiency | $\eta_{exp\,is}$ | % | 70 |
| Maximum evaporating pressure | P_{evap} | bar | 40 |
| Minimum condensing pressure | P_{cond} | bar | 1 |
| Maximum pressure ratio | $\frac{P_{evap}}{P_{cond}}$ | - | 40:1 |
| Pinch points HEX | PP | K | 10 |
| Pressure ratio among HEX | $\frac{P_{f\,out,\,boiler}}{P_{f\,out,\,pump}}$ | - | 1 |
| Minimum quality after expansion | $x_{f\,out,\,exp,\,min}$ | - | 0.9 |

Table 1: 0D model parameters

135 Refprop database [?] is used to compute the following quantity: h , s , T ,
136 P_{sat} and T_{sat} . Input variables of the model (1) are the gas mass flow and
137 temperature (denoted by \dot{m}_{gas} and $T_{gas\,in,\,boiler}$) entering in the system and
138 the condensing temperature (T_{cond}). Outputs of the model are the power
139 produced by the expansion \dot{W}_{exp} , the power consumed by the compression
140 \dot{W}_{pump} and the net output power NOP which are defined as:

$$\begin{cases} NOP &= \dot{W}_{exp} - \dot{W}_{pump}, \\ \dot{W}_{exp} &= \dot{m}_f * (h_{f\,in,\,exp} - h_{f\,out,\,exp}), \\ \dot{W}_{pump} &= \dot{m}_f * (h_{f\,in,\,pump} - h_{f\,out,\,pump}). \end{cases} \quad (3)$$

141 The model 1 is not dynamic and does not represent any real components
142 performance. A dynamic 1D model is therefore developed to evaluate the
143 system performance on more realistic dynamic driving conditions.

144 3.3. 1D dynamic modeling of a Rankine cycle

145 3.3.1. Tank

146 The reservoir is modeled by a fixed volume, which can be either vented to
147 the atmosphere or be hermetic (depending on the condensing pressure) in
148 order to avoid sub atmospheric conditions. Mass and energy conservation

149 equations are:

$$\left\{ \begin{array}{l} \dot{m}_{f_{out,tank}} - \dot{m}_{f_{in,tank}} = \frac{\partial m_{f_{tank}}}{\partial t}, \\ \dot{m}_{f_{in,tank}} h_{f_{in,tank}} - \dot{m}_{f_{out,tank}} h_{f_{out,tank}} = m_{f_{tank}} \frac{\partial h_{f_{tank}}}{\partial t}. \end{array} \right. \quad (4)$$

150 3.3.2. Working fluid pump

The working fluid pump is simply represented by a fixed displacement and isentropic efficiency. The volumetric efficiency is a function of the outlet pressure. This law is identified thanks to experimental data:

$$\dot{m}_{f_{out,pump}} = \rho_{f_{in,pump}} \frac{N_{pump}}{60} C_{cpump} \eta_{pumpvol}. \quad (5)$$

151 The outlet enthalpy is calculated as shown in the equation for $h_{f_{out,pump}}$ in
152 the 0D model (1).

153 3.3.3. Heat exchangers: Evaporator(s) and condenser(s)

154 The models are developed to dynamically predict temperature and enthalpy
155 of transfer and working fluid at the outlet of each heat exchanger (HEX).
156 When coming to dynamic models of those components, two methodologies
157 can be found in the literature: moving boundary (MB) and finite volume
158 (FV) models. Usually more complex in terms of computational capacity
159 needed due to the high number of system states, the FV approach has the
160 advantage to be more powerful and robust concerning the prediction. Both
161 approaches have been widely used in large power recovery system and control
162 system design [? ? ? ?] and results in a simplification of the heat recovery
163 boiler/condenser geometry in a great extent (i.e. by representing the boiler
164 by a straight pipe in pipe counterflow heat exchanger). In this study, the FV
165 approach is preferred since it easily handles starting and shut down phases
166 [?] when only few papers adressed those cases with a MB approach [?].

167

168 *Model assumptions.* Several assumptions are done to simplify the problem
169 in a great extent. These ones are usually admitted when coming to heat
170 exchanger modeling [? ?]:

- 171 • The transfer fluid is always considered in single phase, i.e. no conden-
172 sation in the EGR/exhaust gases is taken into account.
- 173 • The conductive heat fluxes are neglected since the predominant phe-
174 nomenon is the convection.
- 175 • All HEX are represented by a straight pipe in pipe counterflow heat
176 exchanger of length L .
- 177 • Fluid properties are considered homogeneous in a volume.
- 178 • Pressure dynamics is neglected since it is very fast compared to those
179 of heat exchanger.

180 *Governing equations.* Boiler(s) and condenser(s) models are based on mass
181 and energy conservation principles.

- 182 • Working fluid (internal pipe):

$$\begin{cases} A_{cross_f} \frac{\partial \rho_f}{\partial t} + \frac{\partial \dot{m}_f}{\partial z} = 0, \\ A_{cross_f} \frac{\partial \rho_f h_f}{\partial t} + \frac{\partial \dot{m}_f h_f}{\partial z} + \dot{q}_{conv_{f_{int}}} = 0, \\ \dot{q}_{conv_{f_{int}}} = \alpha_f P e_{exch_f} (T_f - T_{wall_{int}}). \end{cases} \quad (6)$$

- Internal pipe wall: An energy balance is expressed at the wall between the working fluid and the gas and is expressed as follows:

$$\dot{Q}_{conv_{f_{int}}} + \dot{Q}_{conv_{g_{int}}} = \rho_{wall} c_{p_{wall}} V_{wall_{int}} \frac{\partial T_{wall_{int}}}{\partial t}. \quad (7)$$

- Gas side (external pipe): The energy conservation is then formulated under the following form:

$$\rho_g A_{cross_g} c_{p_g} \frac{\partial T_g}{\partial t} + c_{p_g} \dot{m}_g \frac{\partial T_g}{\partial z} + \dot{q}_{conv_{g_{int}}} + \dot{q}_{conv_{g_{ext}}} = 0, \quad (8)$$

183 where the convection on the external side is used to represent the heat
184 losses to the ambient.

- External pipe wall: As for the internal pipe an energy balance is expressed between the gas and the ambient:

$$\dot{Q}_{conv_{g_{ext}}} + \dot{Q}_{conv_{amb_{ext}}} = \rho_{wall} c_{p_{wall}} V_{wall_{ext}} \frac{\partial T_{wall_{ext}}}{\partial t}. \quad (9)$$

185 In equation (7) and (9) the convection heat flow rate (\dot{Q}_{conv}) is expressed as:

$$\dot{Q}_{conv_{jk}} = \alpha_j A_{exch_{jk}} (T_{wall_k} - T_j), \quad (10)$$

where $j = g, f, amb$
and $k = int, ext$.

186 Furthermore, to complete the system, one need boundary and initial condi-
187 tions. Time-dependent boundary conditions are used at $z = 0$ and $z = L$
188 ($t > 0$):

$$\dot{m}_f(t, 0) = \dot{m}_{f_0}(t), \quad (11)$$

$$h_f(t, 0) = h_{f_0}(t), \quad (12)$$

$$\dot{m}_g(t, L) = \dot{m}_{g_L}(t), \quad (13)$$

$$\dot{T}_g(t, L) = T_{g_L}(t). \quad (14)$$

189 The initial conditions for the gas and wall temperatures and working fluid
190 enthalpy are given by ($z \in [0, L]$):

$$h_f(0, z) = h_{f_{init}}(z), \quad (15)$$

$$T_{wall_{int}}(0, z) = T_{wall_{int_{init}}}(z), \quad (16)$$

$$T_g(0, z) = T_{g_{init}}(z), \quad (17)$$

$$T_{wall_{ext}}(0, z) = T_{wall_{ext_{init}}}(z), \quad (18)$$

Heat transfer and pressure drop. To model the convection from the transfer fluid to the pipe walls and from the internal pipe to the working fluid, a heat transfer coefficient (α) is needed. The convection from a boundary to a moving fluid is usually represented by the dimensionless number Nusselt (Nu) which is the ratio of convective to conductive heat transfer.

$$Nu(\alpha) = \frac{\alpha l}{\lambda}, \quad (19)$$

where l represents a characteristic length and is, in this case, the hydraulic diameter. Numerous correlations to approach this number can be found in the literature and are usually derived from experiments, see for example [?]. In single phase, the Gnielinski correlation is chosen for both fluids. In two phase, Chen (for evaporation) and Shah (for condensation) correlations are used. Pressure drop in both fluids are taken into account in order to simulate

the real performance of the system. The pressure drop can be split into three main contributors:

$$\Delta P = \Delta P_{static} + \Delta P_{momentum} + \Delta P_{friction}, \quad (20)$$

191 where the static pressure drop (ΔP_{static}) is function of the change in static
 192 head (i.e. the height), the momentum pressure drop ($\Delta P_{momentum}$) depends
 193 on the change on density during phase change and the friction contribution
 194 ($\Delta P_{friction}$) is function of the speed of the fluid and the considered geometry.
 195 Table 2 shows the different correlations used depending on flow conditions.
 196 In laminar single phase, the assumption of a constant heat flux at the wall
 is made.

| | | Laminar | Turbulent |
|---------------|------------------------|------------|------------|
| Heat transfer | Single phase | Nu = 4.36 | Gnielinski |
| | Two phase evaporation | Chen | Chen |
| | Two phase condensation | Shah | Shah |
| Pressure drop | Single phase | Poiseuille | Blasius |
| | Two phase | Friedel | Friedel |

Table 2: Correlations used in HEX

197

198 3.3.4. Valve(s)

The fluid flow \dot{m} through the valve is modeled using a compressible valve equation of the form:

$$\dot{m}_{f_{in,v}} = C_{d_v} S_{eff_v} \sqrt{\rho_{f_{in,v}} P_{f_{in,v}} \phi}, \quad (21)$$

199 where the compressibility coefficient ϕ is defined as:

$$\phi = \frac{2\gamma_f}{\gamma_f - 1} \left(\varphi^{\frac{2}{\gamma_f}} - \varphi^{\frac{\gamma_f+1}{\gamma_f}} \right), \quad (22)$$

with

$$\varphi = \begin{cases} \frac{P_{f_{out,v}}}{P_{f_{in,v}}} & \text{if } \frac{P_{f_{out,v}}}{P_{f_{in,v}}} > \frac{2}{\gamma_f+1} \frac{\gamma_f}{\gamma_f-1} \\ \frac{2}{\gamma_f+1} \frac{\gamma_f}{\gamma_f-1} & \text{if } \frac{P_{f_{out,v}}}{P_{f_{in,v}}} \leq \frac{2}{\gamma_f+1} \frac{\gamma_f}{\gamma_f-1}, \end{cases} \quad (23)$$

200 where γ_f is the ratio of the specific heats of the working fluid and depends on
 201 the temperature and the pressure. Equation (23) means that the parameter
 202 φ is either the pressure ratio if the flow is subsonic or the critical pressure
 203 ratio when the flow is supersonic.

204 3.3.5. Expansion machine

Several studies have been carried out in order to choose the correct expansion machine for Rankine based recovery system [? ?]. In most of them where vehicle installation is considered, turbine expanders are preferred for their compactness and their good performance [? ?] since the major advantage of volumetric expander such as piston machines is the expansion ratio [?]. Though, recent study [?] has shown turbine with expansion ratio over 40:1 on a single stage with really good performance at tolerable speed for a vehicle installation. In this study, only a kinetic expander is modeled. The turbine nozzle is represented by the following equation:

$$\dot{m}_{f_{in,exp}} = K_{eq} \sqrt{\rho_{f_{in,exp}} P_{f_{in,exp}} \left(1 - \frac{P_{f_{in,exp}}}{P_{f_{out,exp}}}\right)^{-2}}. \quad (24)$$

205 And the isentropic efficiency is calculated according to the following relation:

$$\eta_{exp_{is}} = \eta_{exp_{is_{max}}} \left(\frac{2c_{us}}{c_{us_{max}}} - \frac{c_{us}}{c_{us_{max}}} \right)^2, \quad (25)$$

where

$$c_{us} = \frac{u}{c_s} = \frac{\omega_{exp} R_{exp}}{2\sqrt{h_{f_{in,exp}} - h_{f_{in,exp_{is}}}}}. \quad (26)$$

206 Model parameters are fitted using data from supplier and similarity relation
 207 [?].

208 3.3.6. Other heat exchanger(s)

In order to describe the vehicle cooling system, the number of transfer unit (NTU) approach is used. It is commonly adopted when it comes to single phase heat exchanger modeling. For an air cooled radiator the following relations are used:

$$\dot{Q}_{air} = \dot{m}_{air} c_{p_{air}} \varepsilon (T_{coolant_{in}} - T_{air_{in}}). \quad (27)$$

209 For a given geometry, ε can be calculated using correlations based on the heat
 210 capacity ratio. By considering parallel flow configuration for the radiators,
 211 the effectiveness can be written:

$$\varepsilon = \frac{1 - e^{-NTU \left(1 + \frac{(\dot{m}c_p)_{min}}{(\dot{m}c_p)_{max}}\right)}}{1 + \frac{(\dot{m}c_p)_{min}}{(\dot{m}c_p)_{max}}}, \quad (28)$$

$$\text{with } NTU = \frac{UA}{(\dot{m}c_p)_{min}}. \quad (29)$$

212 3.3.7. Coolant pump and fan

The coolant pump model used is a map-based model function of engine speed and pressure rise. This one is sized to deliver enough subcooling even at high engine load. The engine fan is also a map-based model delivering a given mass flow at a given speed. The fan consumption is calculated according to:

$$\dot{W}_{fan} = C_{fan} \rho_{air} N_{eng} G_{ratio} N_{fan}^2, \quad (30)$$

where the coefficients C_{fan} and G_{ratio} are dependent on the fan model and vehicle. The mass flow rate blown by the fan is mapped according to data from supplier and depends on the fan speed and atmospheric conditions. The air mass flow rate going through the cooling package (\dot{m}_{air}) is a combination of the natural air mass flow rate (corresponding to a fraction of the vehicle speed) and the forced mass flow rate (corresponding to the mass flow blown by the fan).

$$\dot{m}_{air} = \rho_{air} A_{cool \ pack} S r_{air} V_{vehicle} + \dot{m}_{fan}(N_{fan}, \rho_{air}), \quad (31)$$

213 where $S r_{air}$ is the ratio between the vehicle speed and the air speed in front
 214 of the cooling package and is either calculated via CFD or measured in a
 215 wind tunnel.

216 4. SYSTEM OPTIMIZATION

217 4.1. Key aspects

218 In this section, the degrees of freedom used to optimize the WHRS are de-
 219 tailed:

- 220 1. Fluid choice: the fluid selection is a critical part of the system opti-
221 mization. The correct fluid choice has to match both heat source and
222 cold sink in order to generate as much power as possible [? ?]. From
223 environmental and legal points of view, the working fluid has to respect:
- 224 • Its chemical class: chlorofluorocarbons (CFCs) have been ban-
225 ished by the Montreal Protocol and hydrochlorofluorocarbons (HCFCs)
226 production is planned to be phased out by 2030.
 - 227 • Its presence on the global automotive declarable substance list
228 (GADSL).
 - 229 • Its chemical properties such as the global warming potential (GWP),
230 the ozone depletion potential (ODP) or the risk phrases (R-phrases).
 - 231 • Its classification according the national fire protection agency (NFPA)
232 704 classification (ranking above 1 in Health or Instability class)

233 In top of that, the freezing point which has to be below 0 °C.

- 234 2. Components choice and design: the correct choice of components and
235 particularly the expansion machine have an important impact on the
236 system performance and the control design. Indeed, a volumetric ex-
237 pander is less stringent in terms of degree of superheat and tolerate
238 a given amount of liquid during the expansion process whereas a kinetic
239 expander requires a higher degree of superheat in order to have a full
240 vapor expansion (liquid droplets can cause blade erosion and broke the
241 machine). The design of all other components of the Rankine system
242 is also critical to maximize its potential. For example, too big heat
243 exchangers show higher performance but also inertia which could be a
244 disadvantage when coming to highly dynamic driving cycle since the
245 more interesting points (i.e. high load engine operating points) are not
246 lasting for long. A heavy evaporator is therefore not catching up the
247 maximum potential of this high heat flow rate.
- 248 3. Heat sources and sinks arrangement: the architecture of sources and
249 sinks has to be adapted to increase overall performance. Heat sources
250 choice and arrangement impact a lot the system performance by chang-
251 ing the heat input to the system. The cold sinks choice is influencing
252 the condensing pressure so the overall pressure ratio (and therefore the
253 power generated by the expander).

254 4. Other system interactions: as the final goal is to implement the system
 255 in a heavy duty vehicle, the WHRS must be considered not as a stand-
 256 alone system but as a connected sub system of the complete vehicle.
 257 The interactions of the Rankine system on the other sub-systems have
 258 to be taken into account (e.g. increase in fan consumption due to the
 259 heat rejection coming from the condenser).

260 *4.1.1. Investigated architectures and components*

261 Several studies have been conducted in the field of waste heat recovery Rank-
 262 ine based systems for mobile applications. A screening of the different heat
 263 sources available is reported in [?] and shows that the most promising ones
 264 are the EGR and the Exhaust streams. In the present study, only these
 265 two heat sources are considered since they present the higher grade of tem-
 266 peratures among other sources. Therefore four different Rankine layout are
 267 studied:

- 268 1. Exhaust recovery only where the only heat source are the exhaust gases.

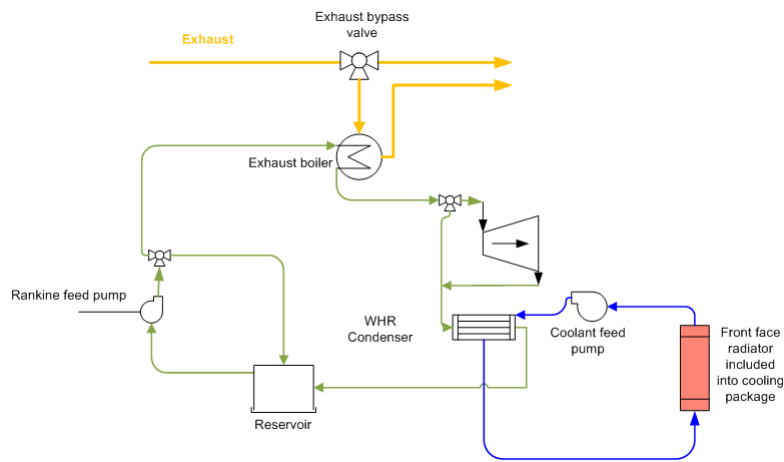


Figure 3: Exhaust only system schematic

- 269 2. EGR recovery only where only the EGR gases are used as the only heat
 270 source.

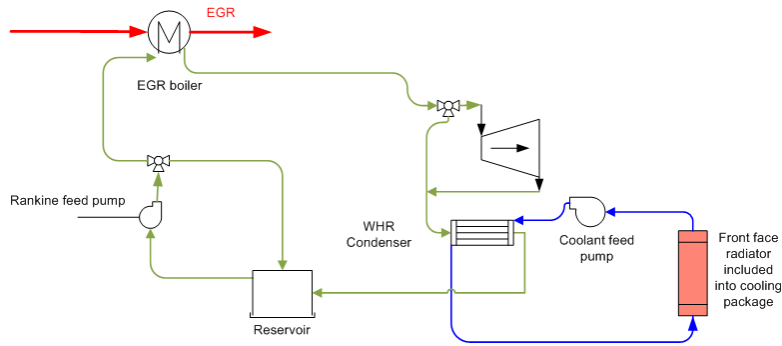


Figure 4: EGR only system schematic

- 271 3. Both sources in parallel where the working fluid is split into two streams
 272 heated up separately by each source and then mixed before the ex-
 273 pander.

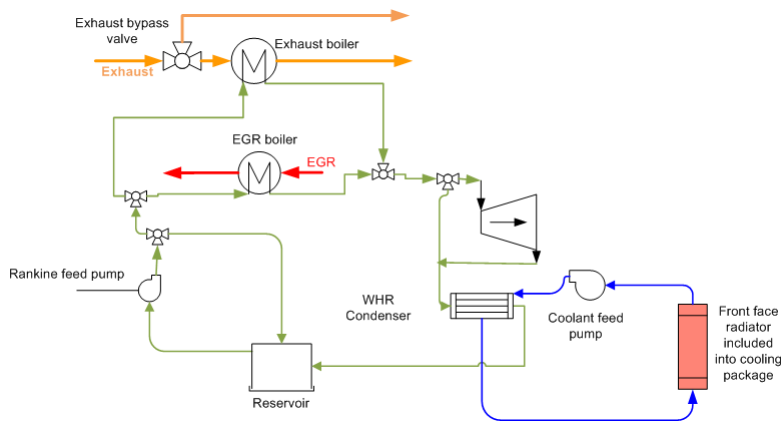


Figure 5: Exhaust and EGR in parallel system schematic

- 274 4. EGR and exhaust in series where the EGR gases are used to preheat
 275 the fluid and the exhaust gases to vaporize and superheat. Using the
 276 EGR as a preheater, instead of a superheater, is chosen to lower the
 277 EGR gases temperature after the evaporation process.

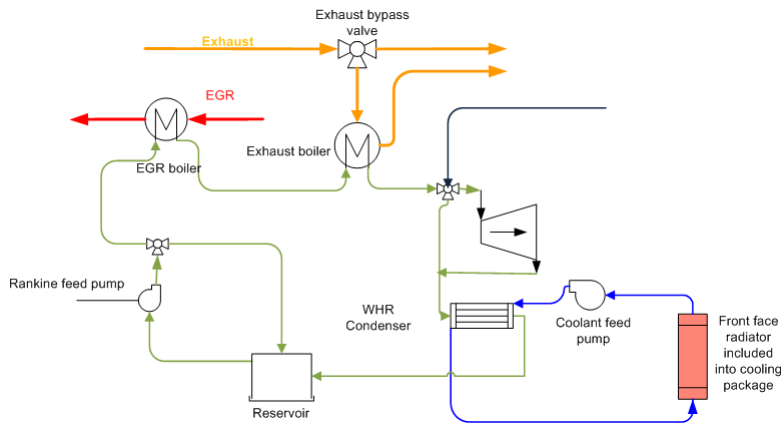


Figure 6: Exhaust and EGR in series system schematic

278 Coupled to that, two different cooling architecture are approached:

- 279 • A first one (called in the following Cooling Config 1) which uses a low
 280 temperature radiator dedicated to the Rankine condenser and is placed
 281 between the charge air cooler (CAC) and the engine radiator.

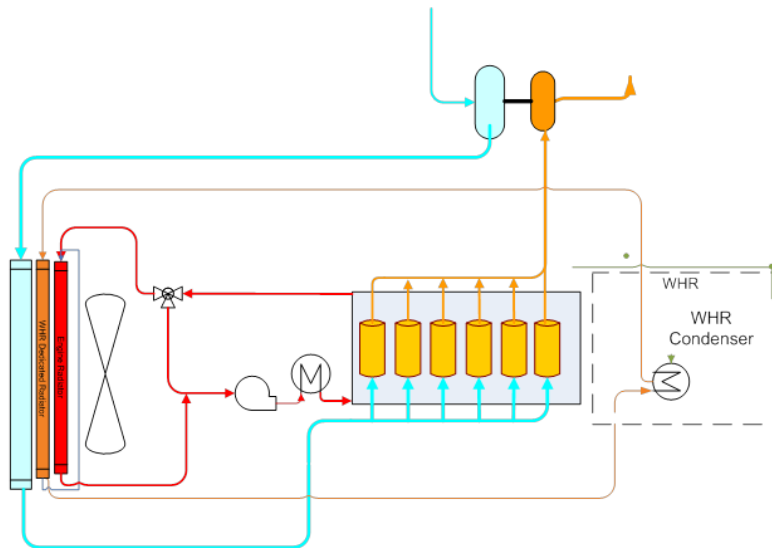


Figure 7: Cooling config 1

- 282 • A second one (called in the following Cooling Config 2) using the engine

283 coolant as heat sink for the Rankine cycle. In that case, a derivation
 284 of the coolant is done in front of the engine to benefit from the lowest
 285 temperature grade.

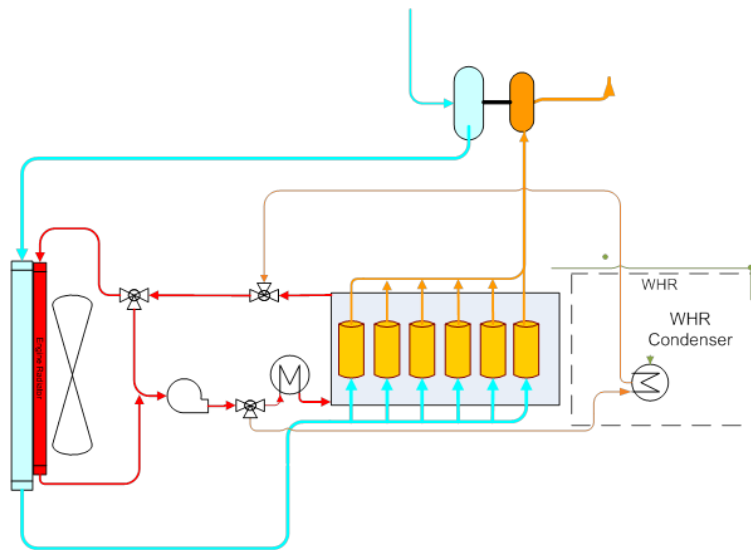


Figure 8: Cooling config 2

286 Concerning the components, as previously said, the study is limited to one
 287 expansion machine technology: turbine expander. For the heat exchangers
 288 (evaporator(s) and condenser), only counter-current configurations which are
 289 usually used in this kind of applications [?] are considered.

290 4.2. Duty cycles

291 Driving conditions are acting as input disturbances and therefore, their im-
 292 pact on the target performance must be studied with care.

293 4.2.1. Steady state evaluation

294 Under steady state driving conditions, the performance is evaluated by ex-
 295 pressing the weighted average net output power of the 1D model (3.3) (the
 296 NOP, which is the additional power that the engine receives, therefore cor-
 297 responds to the fuel economy) on 13 engine operating points (summarized

| Name | Vehicle speed | EGR mass flow | EGR temperature | Exhaust mass flow | Exhaust temperature | Weight factor |
|-----------|---------------|-----------------|-----------------|-------------------|---------------------|---------------|
| Parameter | $V_{vehicle}$ | \dot{m}_{egr} | T_{egr0} | \dot{m}_{exh} | T_{exh0} | w_i |
| Unit | km/h | g/s | $^{\circ}C$ | g/s | $^{\circ}C$ | $\%$ |
| 1 | 20 | 31.5 | 263.1 | 78.7 | 237.9 | 6.9 |
| 2 | 85 | 38 | 409.5 | 119.8 | 338.2 | 9.0 |
| 3 | 60 | 59.5 | 635.0 | 309.3 | 443.9 | 4.9 |
| 4 | 85 | 54.6 | 544.0 | 252.4 | 413.0 | 2.6 |
| 5 | 75 | 46.1 | 454.0 | 154.6 | 366.4 | 18.9 |
| 6 | 85 | 56.3 | 247.5 | 85.7 | 212.5 | 10.5 |
| 7 | 30 | 85.9 | 631.0 | 352.7 | 425.1 | 2.8 |
| 8 | 85 | 69.4 | 562.5 | 290.5 | 405.5 | 3.6 |
| 9 | 50 | 58 | 473.0 | 183.2 | 336.2 | 12.7 |
| 10 | 85 | 59.8 | 251.0 | 95.2 | 216.0 | 11.2 |
| 11 | 45 | 87.1 | 581.0 | 326.8 | 400.8 | 2.3 |
| 12 | 75 | 68.9 | 472.0 | 198.4 | 359.6 | 10.7 |
| 13 | 85 | 62.9 | 252.5 | 102.8 | 217.5 | 3.9 |

Table 3: Steady state evaluation: Driving conditions and weight for 13 engine operating points

298 in table 3) These operating points are chosen to represent a classical long
299 haul driving cycle and weighted according to the percentage of energy used
300 on each operating point. Operating point number 5 is identified as the de-
301 signing point whereas the operating points 3 and 11 are considered critical
302 due to the high engine load and the low vehicle speed.

303 4.2.2. Dynamic evaluation

304 In order to accurately assess the potential of the WHRS, dynamic driving cy-
305 cles are also used to complete the study and check whether the performance
306 found with the previous method is correct. This is really important when
307 coming to thermal systems performance estimation since they generally have
308 long response time [?]. The driving cycle used is split into 7 phases (sum-
309 marized in table 4) supposed to represent all conditions of a long haul truck
310 usage.

| Driving cycle | 1 | 2 | 3 | 4 | 5 | 6 | 7 |
|-------------------------|-------------|---------|---------|-------------|-------------|-------------|---------|
| Road Type | Extra urban | Highway | Highway | Extra urban | Extra urban | Extra urban | Rolling |
| Vehicle speed | Medium | High | Medium | Low | Medium | High | High |
| Weight factor w_i (%) | 10 | 10 | 50 | 7.5 | 10 | 7.5 | 5 |

Table 4: Dynamic evaluation: Driving conditions and weight for the 7 phases

311 In the previous 1D model (3.3), each phase is considered, in the rest of the
312 study, as a driving cycle of approximately the same length (denoted by a
313 number from 1 to 7) and weighted according to their real life importance
314 (for a long haul truck highway is predominant).

315 4.3. System performance evaluation

The criterion used for the performance evaluation under steady state and dynamic driving conditions, is the total net reinjected power to the conventional driveline. This is done by taking into account the producer (WHRS expander) and different consumers (cooling fan, WHRS pump and WHRS coolant pump) and assuming them to be mechanically driven (this is not always true for the pumps but efficiencies are detuned to take into account the mechanical to electrical conversion). A complete vehicle model integrating engine, EATS, transmission, cooling package, WHRS and road environment is used to simulate the total vehicle approach and calculate the power needed to drive the vehicle. The performance criterion (PC) is then calculated as the ratio of this reinjected power to the engine power:

$$PC_i = \int_{t_{init}}^{t_{final}} \frac{\dot{W}_{exp} - \dot{W}_{pump} - \dot{W}_{cool,pump} - \dot{W}_{fan}}{\dot{W}_{eng}}, \quad (32)$$

where the engine power (\dot{W}_{eng}) taking into account the mechanical auxiliaries consumption mounted on it and the increase in exhaust backpressure (due to the exhaust evaporator). The vehicle gross weight is assumed constant and equal to 36 tons which intends to represent the average load on a long haul truck. The performance criterion (PC) over the different steady state operating points or driving cycles is then calculated by summing the weighted

PC on each points/cycles:

$$PC = \sum_{i=1}^k w_i PC_i, \quad (33)$$

316 where $k \in [1 \ 13]$ for steady state evaluation (presented in section 4.2.1) and
317 $k \in [1 \ 7]$ for evaluation on dynamic driving cycle (presented in section 4.2.2).

318 5. RESULTS AND DISCUSSION

319 5.1. 1D model validation

320 In this section some component models, judged as critical for the overall
321 system performance evaluation, are first validated thanks to supplier or ex-
322 perimental data. The different studied configurations being made of the same
323 components model it has been decided to validate the models components by
324 components. The validation is done by comparing experimental to the mod-
325 eling results. A model is further considered as valid if the average modeling
326 error is below 5% of the predicted quantity. Since the main dynamic of the
327 system is contained in the evaporators [?] and the final aim is to predict
328 the power generated by the system only validation figures are presented for
329 the evaporators and the expansion machine. It should be said that a more
330 detailed validation on the whole system mounted on the vehicle should be
331 carried out but this requires the system to be built. Unfortunately this tech-
332 nology is still under investigation at the truck makers level and no figures
333 are available yet. This study intends then to compare the architecture and
334 analyze their impact on the truck fuel consumption.

335 5.1.1. Heat exchangers

336 A high attention is paid to the evaporators in order to accurately predict the
337 steady state and dynamic performance of those components (corresponding
338 to the model presented in section 3.3.3). In this paper, a finite volume ap-
339 proach has been chosen to implement the continuous set of equations (equa-
340 tions 6, 7, 8, 9). Figure 9 shows the schematic of the discretized model.
341 Table 5 and 6 show respectively steady state and dynamic prediction errors.
342 Note that in both cases the relative error is computed according to the max-
343 imum temperature difference between the heat exchanger bounds (usually

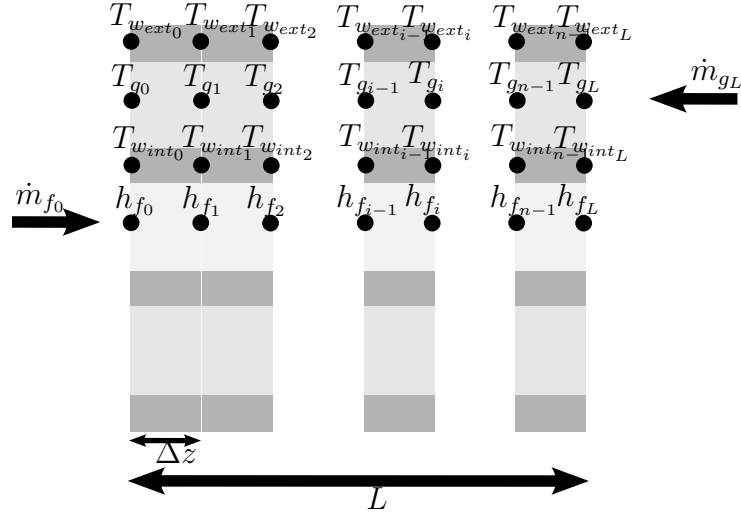


Figure 9: HEX model schematic

344 $T_{gL} - T_{f0}$). The steady state validation is conducted on a lot of operating
 345 conditions supposed to represent the complete range of operation for those
 346 components. The dynamic behavior is evaluated on different load point varia-
 347 tions but obviously need further validation especially on fast change that can
 348 take place on real driving conditions. However, the mean relative modeling
 349 error remains lower than 3.5%, which is considered acceptable.

| | $T_{fL_{EGRB}}$ | | $T_{fL_{ExhB}}$ | | $T_{egr0_{EGRB}}$ | | $T_{exh0_{ExhB}}$ | |
|--------------|-----------------|------|-----------------|------|-------------------|------|-------------------|------|
| Error | max | mean | max | mean | max | mean | max | mean |
| Absolute (K) | 2.95 | 1.30 | 9.15 | 4.16 | 7.54 | 2.54 | 15.47 | 4.71 |
| Relative (%) | 0.57 | 0.29 | 8.84 | 3.28 | 2.34 | 0.61 | 8.61 | 3.40 |

Table 5: Evaporators steady state validation

| | $T_{fL_{EGRB}}$ | | $T_{fL_{ExhB}}$ | | $T_{egr0_{EGRB}}$ | | $T_{exh0_{ExhB}}$ | |
|--------------|-----------------|------|-----------------|------|-------------------|------|-------------------|------|
| Error | max | mean | max | mean | max | mean | max | mean |
| Absolute (K) | 4.5 | 1.5 | 25.9 | 2.3 | 7.9 | 2.8 | 20 | 4.2 |
| Relative (%) | 1.38 | 0.46 | 14.37 | 1.28 | 2.43 | 0.86 | 11.1 | 2.33 |

Table 6: Evaporators dynamic validation

350 *5.1.2. Expansion machine*

351 The turbine expander model presented in 3.3.5 is fitted thanks to supplier
352 data. Figure 10 and 11 respectively show the working fluid inlet pressure and
353 the generated power predicted by the model versus the normalized working
354 fluid mass flow entering in the turbine. Those two quantities are well fitted
355 and this model is further considered validated.

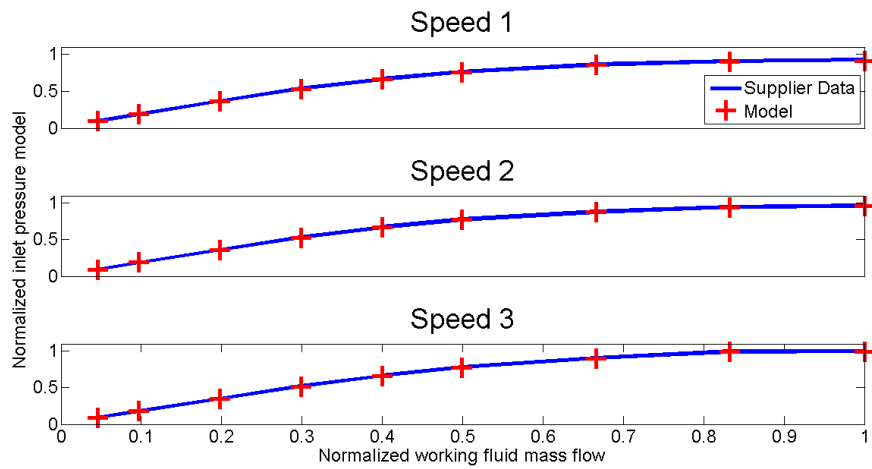


Figure 10: Turbine pressure model validation

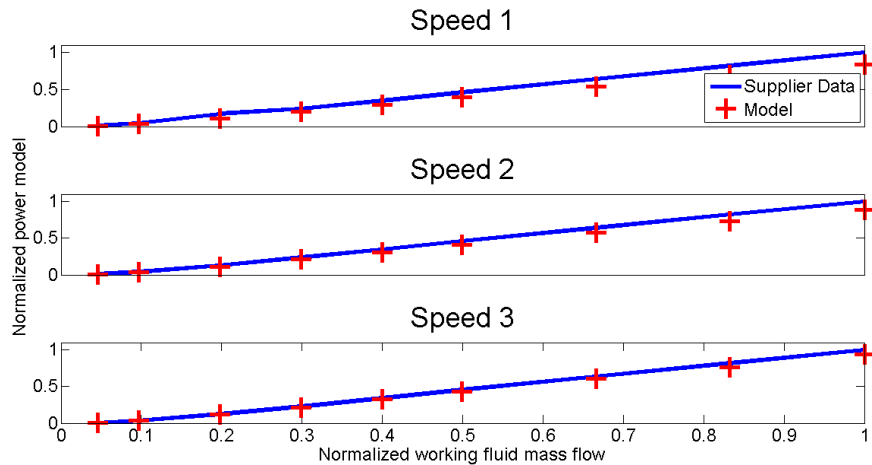


Figure 11: Turbine power model validation

356 5.1.3. Model analysis

357 The whole 1D models are built from the same component models. The iner-
358 tial effect of the pipes are neglected since their effect are negligible compared
359 to the other components dynamics (namely the evaporators) [?]. The full
360 model is then a combination of validated detailed models (e.g. heat exchang-
361 ers) and quasi-static models (pumps expansion machine and fan) used for
362 comparison purpose. This study then intends to compare the different heat
363 sources and sinks configurations possible on a heavy duty vehicle to select
364 the best system in terms of performance.

365 5.2. Optimization of the WHRS

366 5.2.1. Working fluid selection

367 From an exhaustive fluid list [?], all those that do not respect the different
368 criteria mentioned in 4.1 have been removed. However, as water is a good
369 reference fluid since it is generally used in power plant [?], it has been kept.
370 The results presented hereafter are coming from the ideal thermodynamic 0D
371 model presented in section 3.2 where all 13 operating points are simulated for
372 two condensing temperatures 60°C and 90°C, which intends to represent the
373 two cooling configurations presented in the previous section. The parameters
374 of the cycle, $P_{f_{out,pump}}$ and \dot{m}_f are optimized to reach the highest performance
375 (i.e. maximize the *NOP*). Here, each hot stream is simulated separately in
376 order to see the impact of the heat source on the Rankine fluid selection. The
377 simulation matrix contains 13 operating points (listed in section 5.2.2) and
378 13 selected working fluids. For the sake of simplicity, the results presented
379 in figure 12 show the number of occurrences where the fluid is in the top
380 five¹ regarding the *NOP*. When analyzing each operating point and config-
381 uration separately among the 13x13 simulations, water is the best fluid for
382 heavily loaded operating points. For low and medium engine load, as gases
383 temperatures are lower and due to the large enthalpy of vaporization of water
384 and the high level of superheating required, it is not recommended to use it.
385 Acetone and ethanol show good performance at mid and high engine load no
386 matter of the cold sink temperature. Refrigerants such as R1233zd or Novec

¹top five means the *NOP* related to the fluid is ranked in one of the five first position

387 649 show good results for heat source temperature under 280 °C for the low-
 388 est condensing temperature. More exotic fluids such as cis-butene or MM
 389 (silicon oil) could be attractive for low and medium engine load respectively
 390 at 60°C condensing temperature for the first one and 90°C for the second one.

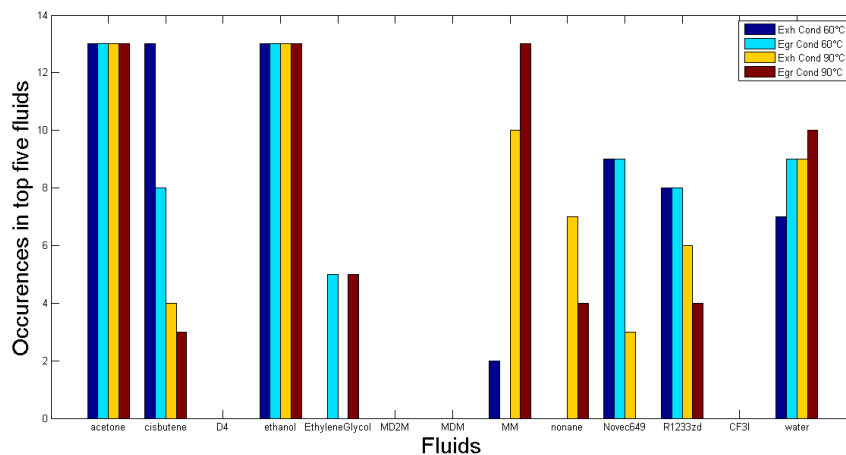


Figure 12: Number of occurrences of each fluid in top five ¹ for different boundary conditions

391

392 These first simulations results limit the number of investigated working fluids
 393 for the remaining part of this paper to the following ones: Acetone, Ethanol.
 394 Those two fluids represent the highest number of occurrences for the differ-
 395 ent configurations considered. As these fluids have similar volumetric flows
 396 it would be possible to use the same components' characteristics with only
 397 some minor changes (e.g. throat diameter for the turbine model and pump
 398 displacement). However due to the low flash point of Acetone (-20°C) only
 399 ethanol is then considered suitable for a mobile application.

400 5.2.2. Steady state performance analysis

401 Now, the performance criterion is analyzed on the 13 operating points and
 402 the 2 cooling architectures (Cooling config 1 and 2) for the previously cho-
 403 sen working fluids. The savings are computed thanks to the weight factors
 404 presented in table 3. Figure 13 presents the NOP to engine power ratio eval-
 405 uated for the 2 cooling configurations. It can be observed that the decrease

406 due to higher condensing temperatures induced by cooling configuration 2 is
407 somehow constant (between 11 and 15 %) no matter of the Rankine cycle
408 arrangement. This drop in performance is due to the increase in condensing
409 pressure which affects the overall pressure ratio through the expansion ma-
410 chine and therefore its performance. This could be partially balanced by a
411 specific design of the expansion machine in order to have a variable nozzle ge-
412 ometry that keeps the pressure ratio constant when the condensing pressure
413 increases. A similar approach is done in [?] to adapt the nozzle geome-
414 try to the mass flow entering in the turbine. With those components, the
415 parallel arrangement of the heat sources gives the best PC , followed by the
416 serial one, the exhaust only and the EGR recovery. However the difference
417 between series and parallel layout is not so important and the lower number
418 of valves needed by the first one could compensate this drop in performance.
419 Moreover, in this configuration, as the working fluid mass flow is controlled
420 to get a superheated vapor state at the outlet of the tailpipe boiler the mass
421 flow rate is then higher than in any other configurations. It results into lower
422 EGR temperature which could be a benefit in terms of engine performance
423 and pollutant emission control [?]. Last but not least, with the EGR only
424 solution even if the weight and installation impact is low (the heaviest com-
425 ponent is the EGR evaporator that replaces the traditional EGR cooler),
426 the PC seems too low for a vehicle installation. This obviously needs further
427 analysis taking into account also the cost impact of each solution on the total
428 cost of ownership.

429 5.2.3. *Dynamic performance analysis*

430 Then, in order to validate the previously used method, dynamic simulations
431 are run to further assess the performance criterion of the WHRS. Indeed,
432 as previously said, the Rankine based recovery systems could have long time
433 constant due to the boiler(s) inertia (wall capacity). This could help in terms
434 of control by filtering some high transient of the heat sources but reduce the
435 heat transferred to the fluid, since only a fraction of the heat contained in
436 the hot gases is then used. In the following, the performance is assessed on 7
437 different driving cycles (see table 4) representative of a long haul truck usage.
438 An example of two of those road profiles is presented in fig 14.

439 Each driving cycle is simulated separately starting from ambient conditions
440 that can result in a lower PC due to the long warm up time of the exhaust

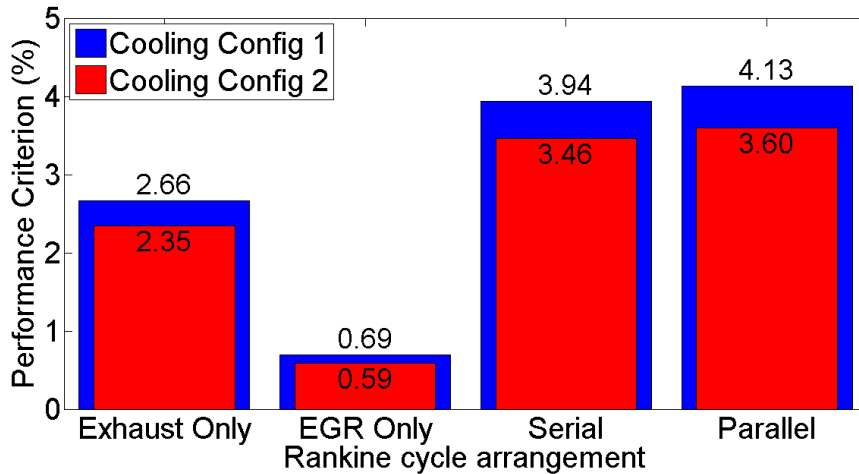


Figure 13: Steady state *PC* assessment

441 after treatment system (EATS). Weights (see 4) are applied to the different
 442 driving cycles to calculate the total performance criterion of the WHRS.
 443 Figures 15 and 16 show the *PC* reached by each Rankine configuration re-
 444 spectively for cooling configuration 1 and 2. As shown is 5.2.2 the decrease in
 445 performance using cooling configuration 2 rather than cooling configuration
 446 1 is more or less constant and around 11%. The main information brought
 447 by this study remains the lower fuel savings when simulating the system in
 448 dynamic instead of steady state, which can be as big as 50% for the systems
 449 using exhaust as heat source. This is due to two main reasons:

- 450 • the exhaust after treatment system, which has a very important constant
 451 time, causes big temperature drop during fast highly loaded engine
 452 conditions where a lot of heat is supposed to be available.
- 453 • the non optimal design of the tailpipe boiler used in the simulation
 454 model. Indeed the validation of the model shown in section 5.1 is
 455 based on prototypes components that do not represent the optimum in
 456 terms of size and transient performance.
- 457 • the constraint implemented on the EGR temperature at the evaporator
 458 outlet not to derate the emission control. The maximum EGR temper-
 459 ature is set to 150 °C which on some phases is not going hand in hand
 460 with the superheat level control. The EGR temperature becomes the

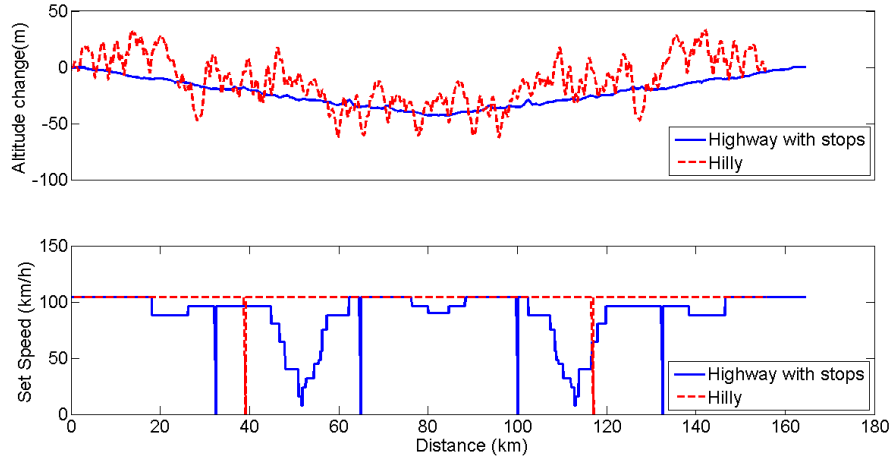


Figure 14: Road profiles examples

461 control objective and when the superheat is not sufficient the expander
 462 is not fed with working fluid and therefore the power production is null.

463 Table 7 resumes the time (relative to the duty cycle time) where the superheat
 464 is sufficient to feed the expansion vapor. Systems recovering heat from the
 465 exhaust stream mainly suffer from a long start-up phase but then the system
 466 never lose the superheat level needed to expand the working fluid in the
 467 kinetic turbine. This long start-up is due to the boundary conditions used
 468 where all the sub-systems initial temperatures are set to ambient. For the
 469 system recovering heat only from the EGR the start-up is not significant since
 470 on some cycles the system is generating power more than 99% of the time
 471 (the EGR gets its normal operation temperature after few seconds whereas
 472 the thermal inertia of the EATS makes the temperature rise very slow).
 473 Nevertheless on highly loaded cycles (namely 3 and 7) the high engine load
 474 results into high EGR temperature and to not interact too much with the
 475 engine emissions system, the superheat is dropped to the detriment of the
 476 EGR temperature. Superheated vapor is no longer generated by the boiler
 477 and the fluid goes back to a diphasic state and the expansion machine is
 478 bypassed.

479 Anyway, similarly to the previous results in steady state, the best system in
 480 terms of fuel savings remains the EGR and exhaust in parallel with cooling
 481 configuration 1 that brings 2.2% savings on the overall weighted driving cycle.

| Driving cycle | Configuration | | | |
|---------------|---------------|--------|--------|----------|
| | Exhaust | EGR | Serial | Parallel |
| 1 | 93.37 % | 99.11% | 93.71% | 93.93% |
| 2 | 93.06% | 99.30% | 93.41% | 93.25% |
| 3 | 95.27% | 83.38% | 95.64% | 95.44% |
| 4 | 92.50% | 93.37% | 91.07% | 92.06% |
| 5 | 91.18% | 97.26% | 90.67% | 91.55% |
| 6 | 92.00% | 98.30% | 90.42% | 91.46% |
| 7 | 93.53% | 88.94% | 90.87% | 92.92% |

Table 7: Vapor creation time ratios summary

482 In addition to that, it can be seen that the relative performance are kept from
arrangement to arrangement (compared to section 5.2.2).

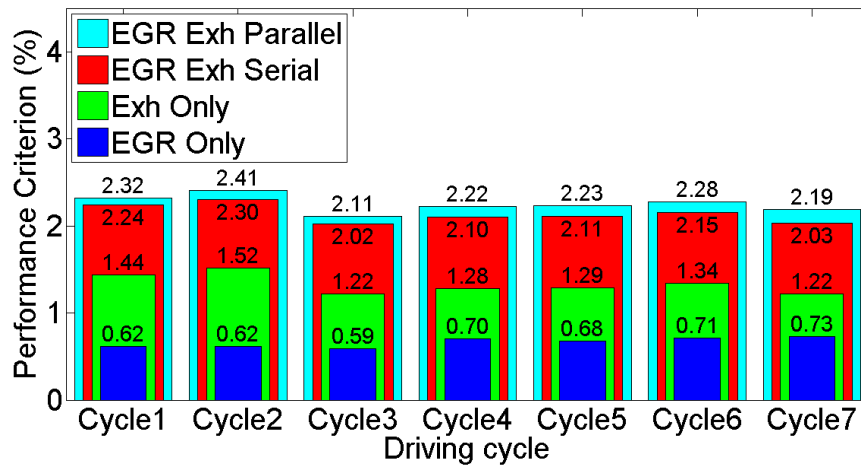


Figure 15: *PC* for cooling configuration 1 over dynamic driving cycles

483

484 5.2.4. Optimal WHRS

485 The low performance figures presented in the previous sections are mainly
486 due to non optimized components for the considered application. In order to
487 evaluate what could be the economy brought by an optimized system, the dif-
488 ferent components constituting the WHRS are redesigned to perfectly match
489 the targeted application. In addition to that, a perfect insulation of these

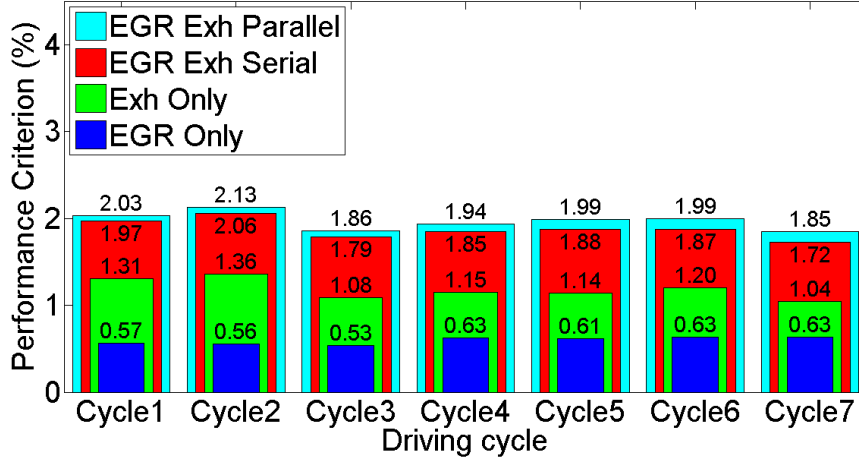


Figure 16: PC for cooling configuration 2 over dynamic driving cycles

490 different components is then considered. In this section, only cooling config-
 491 uration 1 is evaluated since it has been shown that it leads to larger savings.
 492 Both approaches previously used (steady state and dynamic analysis) are
 493 presented in figure 17. Optimization has been done on boilers and condenser
 494 size with respect with the additional weight. Pump and expansion machine
 495 performance are increased to reach standards in power plant Rankine cycles
 496 ($\eta_{pump_{is}} = 70\%$ and $\eta_{exp_{is,max}} = 78\%$). More acceptable results are reached
 497 for a vehicle implementation of such a system, especially when considering a
 498 system recovering from both EGR and exhaust in parallel. Again, a big step
 499 is observed between the two evaluation methodologies which tends to prove
 500 that the cycle division into a certain number of steady state engine operating
 501 points is not adapted for performance evaluation of thermal systems which
 502 generally have a long response time.

503 6. CONCLUSION

504 Performance simulations of different WHRS for heavy duty trucks application
 505 was conducted to understand the potential of such a system in terms of fuel
 506 consumption decrease. Two different methodologies are used and discussed.
 507 Usually, only the first approach, which consists to split a driving cycle into
 508 several steady state engine operating points, is used to assess the performance

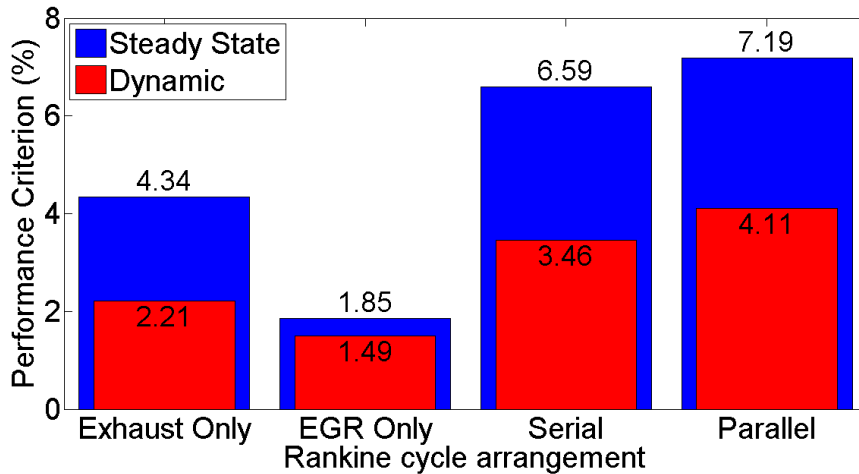


Figure 17: *PC* for optimal sizing of the components

509 without any regards of the transient behavior of the different components
 510 composing the WHRS [?]. The second one, where a total vehicle approach
 511 is simulated over a wide variety of dynamic driving cycles representing the
 512 usage of a long haul HD vehicle. In both methods architecture to architecture
 513 ranking is the same which tends to prove that the first approach could be used
 514 for qualitative but not quantitative study. Using the second approach results
 515 into lower fuel savings and needs to be balanced in regards of the model
 516 validation done based onto prototypes, which are not representing what could
 517 be a mass-produced system. However, the absolute numbers should not be
 518 interpreted as the maximal potential for WHRS in HD trucks, since transient
 519 control of the system and components are not optimal. Different systems
 520 layout have been analyzed to maximize the system performance over a broad
 521 variety of driving cycles. However the results presented in this paper need to
 522 be treated carefully and further completed with the cost and the packaging
 523 effort for each configurations. An optimized scenario is also presented where
 524 a specific attention has been paid to the components size and performance in
 525 order to perfectly match the application. However fuel savings are rather low
 526 compared to what can be found in the literature [? ?] and need to be further
 527 validated by experimental results on a system mounted onto a vehicle. In
 528 addition to that, control issues are not approached in this paper but remain
 529 a big part of the system performance maximization. In this study, perfect
 530 sensors and actuators are used, which reduce the control effort. Moreover,

531 actual mass-produced control units are not as powerful as current laptop
 532 CPU and reduce considerably the possibility in terms of advanced control
 533 algorithm development. Recent studies have brought significant advances
 534 in this field [? ? ?] but this still needs to be addressed when vehicle
 535 implementation is touched.

536 REFERENCES

537 APPENDIX

538 Nomenclature

539 Acronyms

| | | | | | |
|-----|--------------|------------------------------|-----|----------------------|---------------------------------|
| 540 | <i>CAC</i> | Charge air cooler | 561 | γ | Specific heat ratio (–) |
| 541 | <i>CFC</i> | Chlorofluorocarbon | 562 | λ | Heat conductivity ($W/m/K$) |
| 542 | <i>EGR</i> | Exhaust gas recirculation | 563 | ω | Angular velocity (rad/s) |
| 543 | <i>GADSL</i> | Global automotive declarable | 564 | ϕ | Compressibility factor (–) |
| 544 | | substance list | 565 | ρ | Density (kg/m^3) |
| 545 | <i>GWP</i> | Global warming potential | 566 | φ | Critical pressure ratio (–) |
| 546 | <i>HCFC</i> | Hydrochlorofluorocarbon | 567 | Latin letters | |
| 547 | <i>HD</i> | Heavy duty | 568 | \dot{m} | Mass flow (kg/s) |
| 548 | <i>HEX</i> | Heat exchanger | 569 | \dot{Q} | Heat flow rate (W) |
| 549 | <i>NFPA</i> | National fire protection | 570 | \dot{q} | Linear heat flow rate (W/m) |
| 550 | | agency | 571 | \dot{W} | Power (W) |
| 551 | <i>NOP</i> | Net output power | 572 | A | Area (m^2) |
| 552 | <i>NTU</i> | Number of transfer unit | 573 | C_c | Cubic capacity (m^3) |
| 553 | <i>ODP</i> | Ozone depletion potential | 574 | C_d | Discharge coefficient (–) |
| 554 | <i>PC</i> | Performance criterion | 575 | c_p | Specific heat ($J/kg/K$) |
| 555 | <i>WHRS</i> | Waste heat recovery system | 576 | G | Gear ratio (–) |

556 Greek letters

| | | | | | |
|-----|------------|-------------------------------|-----|----------|----------------------------|
| 557 | α | Heat transfer coefficient | 577 | K_{eq} | Equivalent throat diameter |
| 558 | | ($W/m^2/K$) | 578 | | (m^2) |
| 559 | ϵ | Heat exchanger efficiency (–) | 580 | N | Rotational speed (rpm) |
| 560 | η | Efficiency (–) | 581 | Nu | Nusselt number (–) |
| | | | 582 | P | Pressure (Pa) |

| | | | | | |
|-----|-------------------|---------------------------------|-----|--------|---------------------|
| 583 | Pe | Perimeter (m) | 603 | $EgrB$ | EGR boiler |
| 584 | PP | Pinch point (K) | 604 | eng | Engine |
| 585 | r | Ideal gas constant ($J/kg/K$) | 605 | exh | Exhaust gas |
| 586 | S | Section (m^2) | 606 | $ExhB$ | Exhaust boiler |
| 587 | s | Entropy ($J/kg/K$) | 607 | exp | Expander |
| 588 | Sr | Vehicle to ram air speed ratio | 608 | ext | External wall |
| 589 | | ($-$) | 609 | f | Working fluid |
| 590 | T | Temperature (K) | 610 | fan | Cooling fan |
| 591 | t | Time (s) | 611 | g | Gas |
| 592 | V | Volume (m^3) | 612 | in | Inlet port |
| 593 | w | Driving cycle weight ($-$) | 613 | int | Internal wall |
| 594 | x | Quality ($-$) | 614 | max | Maximum |
| 595 | z | Spatial direction (m) | 615 | min | Minimum |
| 596 | Subscripts | | 616 | out | Outlet port |
| 597 | air | Air | 617 | $pump$ | Pump |
| 598 | amb | Ambient | 618 | $tank$ | Tank |
| 599 | $conv$ | Convection | 619 | v | Valve |
| 600 | $cross$ | Cross section | 620 | vol | Volumetric |
| 601 | eff | Effective | 621 | $wall$ | Heat exchanger wall |
| 602 | egr | EGR gas | | | |